ORGANOMETALLICS
Article
Cite This: Organometallics XXXX, XXX, XXX−XXX
pubs.acs.org/Organometallics

Synthesis of Unsymmetrical *N*-Heterocyclic Carbene−Nitrogen−Phosphine Chelated Ruthenium(II) Complexes and Their Reactivity in Acceptorless Dehydrogenative Coupling of Alcohols to Esters

Xiaochun He,[†] Yaqiu Li,[†] Haiyan Fu,[†] Xueli Zheng,[†] Hua Chen,[†] Ruixiang Li,*[,†] and Xiaojun Yu*[,‡]

[†]Key Laboratory of Green Chemistry and Technology of Ministry of Education, College of Chemistry, Sichuan University, Chengdu 610064, China

[‡]Department of Chemistry, School of Basic Medical Sciences, Southwest Medical University, Luzhou 646000, China

Supporting Information

ABSTRACT: Two novel ruthenium complexes RuH(CO)-Cl(PPh_3)(κ^2-CP) (**1**) and [*fac*-RuH(CO)(PPh_3)(κ^3-CNP)]Cl (**2**) bearing unsymmetrical *N*-heterocyclic carbene−nitrogen−phosphine (CNP) were synthesized and characterized with ^{1}H NMR, ^{31}P NMR, and HRMS. The structure of complex **2** was further confirmed by single-crystal X-ray diffraction. An anion exchange experiment proved that complex **2** could transform into complex **1** in solution. The two complexes exhibited a highly catalytic performance in acceptorless dehydrogenative coupling of alcohols to esters, and the excellent isolated yields of esters were given in a catalyst loading of 1% for *para*- and *meta*-substituted benzyl alcohols and long-chain primary alcohols. Although some *ortho*-substituted benzyl alcohols displayed a relatively low reactivity due to the steric hindrance and the coordination of electron donor with the ruthenium center, the good product yields were still obtained by prolonging the reaction time. Especially, this system successfully realized the dehydrogenative cross-coupling to esters between two different primary alcohols.

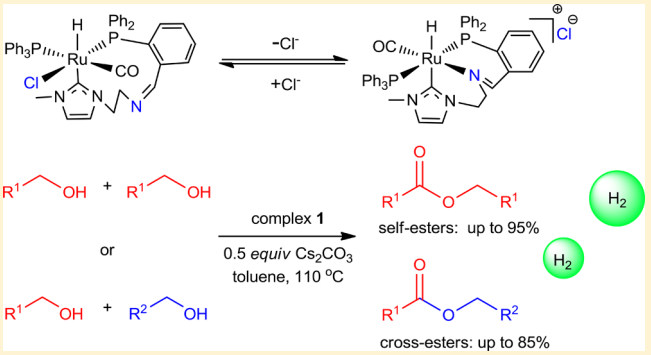

INTRODUCTION

Esters are one of the most important substances and are widely used in the synthesis of food, pharmaceuticals, flavors, coatings, and fragrances.[1,2] The traditional synthetic methods are the esterification of carboxylic acids with alcohols, alcoholysis of acyl halides and anhydrides, oxidation esterification of alcohols, and transesterification of esters with alcohols.[1] However, these methods generally require multistep reactions, stoichiometric strong acids, and toxic strong oxidants, etc..[3] Therefore, to develop new, environmentally benign alternatives for accessing esters from easily available substrates continue to draw the attention of chemists. In this regard, the acceptorless dehydrogenative coupling (ADC) of primary alcohols, in which alcohols as the sole raw material simultaneously produce esters and hydrogen as the only byproduct, has emerged as a safe, environmentally friendly, and atom-efficient process.[4−6]

Usually, the ADC reaction of primary alcohols is conducted with pincer-type complexes as catalysts. Milstein and co-workers achieved a major breakthrough in the field.[6a] Two new heteroaromatic-based pincer ligands chelated Ru(II) hydride complexes efficiently catalyzed the dehydrogenation of primary alcohols to esters under mild conditions.[6a] Beller's group reported that [$Ru(H)_2(CO)[NH(C_2H_4PR_2)_2]$] complexes bearing aliphatic PNP pincer ligands showed significant activity in the catalytic acceptorless dehydrogenation of ethanol to ethyl acetate. Nevertheless, the catalyst would rapidly deactivate without EtONa.[8c] The dehydrogenation of alcohols catalyzed by a series of dihydride Os and Ru complexes was also presented by Gusev et al.[7] Furthermore, other ruthenium pincer-type complexes, bearing symmetric PNP, PCP, unsymmetrical PNN, and PCN-type ligands containing the N−H group, were developed to improve their catalytic activity.[6−10,12,14,15] Among the reported Ru,[6−8] Os,[7,9] Rh,[10] Ir,[11] Fe,[12] Co,[13] Ni,[14] and Mn[15] complexes (Figure 1), ruthenium complexes are the most noticeable ones because they can give high yields of desired products in a low catalyst loading under mild conditions. In fact, based on the concept of metal−ligand cooperation,[16] all ligands in these pincer complexes use pyridine and amino as their backbones, and they chelate with metals in a meridian fashion.[6−9] Additionally, for the access to cross-esterification via the dehydrogenation of alcohols, the successful examples are very rare. Milstein's group reported two elegant works regarding to the acceptorless dehydrogenative cross-esterification, one used PNN-chelated ruthenium(II) complexes between primary alcohols and

Received: February 2, 2019

DOI: 10.1021/acs.organomet.9b00071
Organometallics XXXX, XXX, XXX−XXX

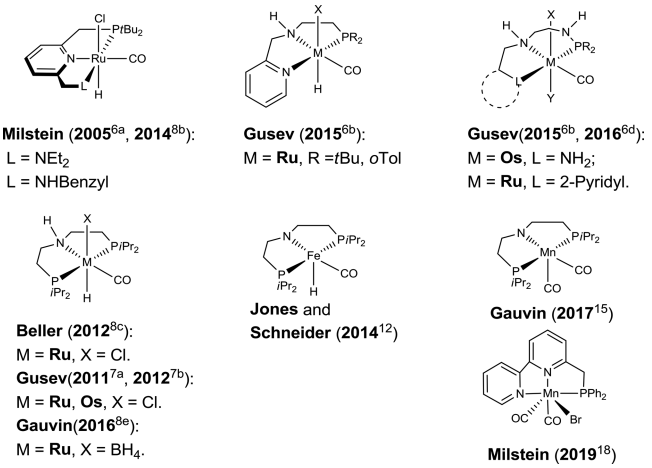

Figure 1. Selected complexes for the ADC reaction.

secondary alcohols, and the other used a manganese pincer complex with benzylic alcohols and different aliphatic alcohols.[17,18] Xiao and co-workers used expensive rhodium complexes to achieve the cross-esterification between substituted benzylic alcohols and aliphatic primary alcohols.[10] Hence, exploring new catalytic systems is a big challenge for the dehydrogenative cross-coupling of the broad alcohol scope to esters and homocoupling.

In the past decades, the introduction of *N*-heterocyclic carbene (NHC) moiety in the flank position of nitrogen and phosphine ligands has attracted great attention because NHC could anchor the metal center by the robust coordination bond, and the potential hemilability of nitrogen or phosphine can provide the coordination vacant site for substrates. The combination of the anchor role of carbene with the hemilability of nitrogen or phosphine could obviously improve the catalyst's stability and activity.[19,20] There are many reports on the synthesis of pincer complexes bearing NHC ligands and their successful application in the transfer hydrogenation,[21,23] CO_2 hydrogenation,[22] Heck coupling,[23b,24] and Suzuki coupling.[23,24] Recently, based on the anchoring role of carbene and hemilability of imine arm, our research group designed and synthesized an unsymmetrical nitrogen−phosphine-functionalized NHC ligand ($\mathbf{L_1}$, Scheme 1). Its palladium complexes displayed a high activity and stability for the arylation of benzoxazoles.[25]

For the sake of making a thorough inquiry in the potentially catalytic performance of ruthenium complexes bearing NHC−nitrogen−phosphine (CNP) $\mathbf{L_1}$, we further synthesized novel complexes $RuHCl(CO)(PPh_3)(\kappa^2\text{-CP})$ and [*fac*-$RuH(CO)(PPh_3)(\kappa^3\text{-CNP})$]Cl and explored their application for the ADC reaction of primary alcohols. To the best of our knowledge, this is the first ruthenium complex bearing a new flexible pincer ligand with a flank NHC moiety (**1** and **2**, Scheme 1) for the direct dehydrogenative coupling of primary alcohols to esters. Although our ligand, coordinated with ruthenium in a facial fashion instead of a meridian one, apparently different from previously reported models,[6,8] the ruthenium complexes not only gave high isolated yields of 85−95% for the homo-esterification of substituted benzyl alcohols and long-chain primary alcohols but also showed middle to good chemoselectivity for the dehydrogenative cross-esterification between benzylic alcohols and aromatic alcohols or branched aliphatic alcohols.

RESULTS AND DISCUSSION

Synthesis of Ruthenium Complexes. The mixture of ligand $\mathbf{L_1}$ and Ag_2O in dichloromethane was stirred at room temperature for 2 h, and then the dichloromethane solution was filtered. The filtrate was added to anhydrous diethyl ether to precipitate Ag complex. Subsequently, the silver complex reacted with $RuHCl(CO)(PPh_3)_3$ in toluene at 60 °C to form the desired product as a pale yellow powder in 71% yield (Scheme 1). The high-resolution mass spectrometry displayed that the accurate molecular weight of the product was in good agreement with that of complex $RuHCl(CO)(PPh_3)(CNP)$. However, the characteristic signals of hydride in this complex showed two groups of peaks at −12.04 ppm and −7.55 ppm in the ^1H NMR spectrum. Similarly, the ^{31}P NMR spectrum also gave two sets of doublets. One was located at 47.0 and 42.7 ppm, and the other was at 40.7 and 36.8 ppm. Obviously, the product was composed of two isomers of $RuHCl(CO)(PPh_3)(CNP)$. It is postulated that the difference between the two isomers might be due to the coordination and dissociation of the nitrogen atom in the imide group according to our previous report.[25] To our delight, pure complex **1** was isolated by column chromatography. The hydride of complex **1** in ^1H NMR spectrum (Figure S1) gave rise to double doublets at −12.04 ppm with coupling constants of 24.2 and 14.3 Hz, which was attributed to the coupling of two phosphorus atoms occupying the *cis* position of the hydride. Furthermore, ^{31}P NMR of complex **1** (Figure S2) exhibited two doublets at 40.7 and 36.8 ppm with a coupling constant of 30.8 Hz. The small coupling constant suggested that two phosphorus atoms in complex **1** were mutually located in the *cis* position. Meanwhile, the characteristic proton signal ratio of imine moiety at 8.64 ppm to the hydride at −12.04 ppm was 1:1 in

Scheme 1. Synthetic Routes of Ruthenium Complexes

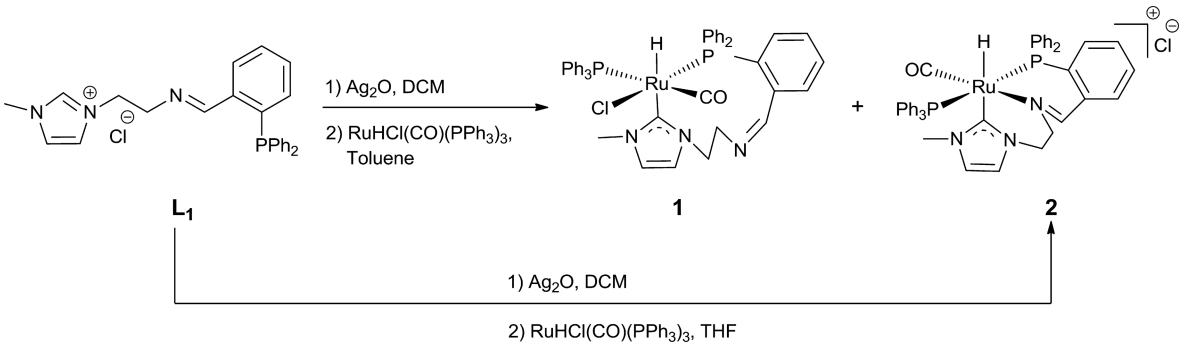

DOI: 10.1021/acs.organomet.9b00071
Organometallics XXXX, XXX, XXX−XXX

the ^{1}H NMR spectrum. The previous NMR spectra revealed that the ruthenium center contained a triphenylphosphine, hydride, and $\mathbf{L_1}$. Complex **2** was obtained by refluxing THF and purified by column chromatography. The hydride in the ^{1}H NMR spectrum exhibited double doublets with coupling constants of 24.8 and 22.0 Hz at −7.55 ppm (Figure S3), which indicated that the hydride was located in the *cis* position of two phosphorus atoms. The ^{31}P NMR spectrum (Figure S5) showed two doublets at 47.0 and 42.7 ppm with a coupling constant of 254.3 Hz. The large coupling constant of phosphorus to phosphorus indicated that two phosphorus atoms in complex **2** were mutually located in the *trans* position. Fortunately, the single crystal of complex **2** was obtained, and its structure was determined by X-ray diffraction (Figure 2).

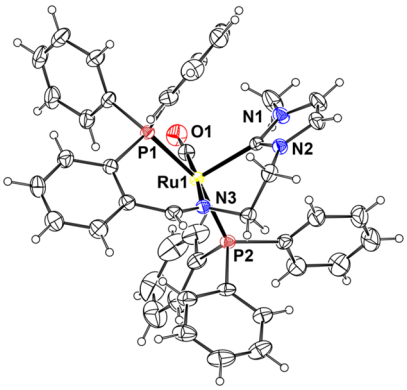

Figure 2. Crystal structure of κ^3-CNP−Ru complex **2**. (**2**·CH_2Cl_2, CH_2Cl_2, H_2O, and chloride ion were omitted for clarity.) Ellipsoids are shown at the 50% probability level. Selected bond lengths (Å): Ru1-C1 = 2.179(5), Ru1-N3 = 2.178(4), Ru1-P1 = 2.3147(13), and Ru1-P2 = 2.3791(13). Selected bond angles (°): N3-Ru1-C1 = 84.36(18), N3-Ru1-P1 = 83.33(11), N3-Ru1-P2 = 92.72(11), P1-Ru1-P2 = 161.32(5), C1-Ru1-P1 = 97.69(13), and C1-Ru1-P2 = 100.09(13).

The six coordination atoms around the ruthenium center featured a slightly distorted octahedral configuration, and the chelating mode of unsymmetrical CNP was in a facial configuration, being different from the ruthenium complexes in a meridional fashion reported by Milstein et al.[8] The terminal carbonyl was located in the *trans* position of the nitrogen atom. PPh_3 was arranged in the *trans* position of the PPh_2 moiety in CNP. The hydride occupied the *cis* position of two phosphorus atoms and was in the *trans* position of the carbene carbon atom, which was in good agreement with the results of ^{31}P NMR and ^{1}H NMR spectra of complex **2**. The bond angle (84.36°) of N3-Ru1-C1 is smaller than that of N3-Ru1-P1 (83.33°) (Table S2), but both angles were obviously smaller than 90° of a standard octahedron. In addition, C1-Ru1-P1 of 97.69° was much larger than 90°. Such a geometric structure made it difficult to form two stable chelating rings due to the torsion tension of chelating bicyclo determined by a dihedral angle of 61.10°. The bond lengths of Ru1-C1, Ru1-N3, Ru1-P1, and Ru1-P2 in complex **2** were 2.18, 2.18, 2.31, and 2.38 Å, respectively (Table S3). Especially, the bond length of Ru1-C1 (2.18 Å) was shorter than that of Ru-C (2.24 Å) in the ruthenium complex chelated by PCP.[8d] The result indicated that a stronger coordination bond between the carbon atom of the NHC moiety and ruthenium was favored to stabilize the catalytic species in the catalytic cycle.

Structure Transformation of Complex 2 to Complex 1. In order to clarify whether complex **2** in solution could transform to complex **1** or not, lithium chloride of 10 equivalents was introduced into the DMSO-d_6 solution of complex **2** (Scheme 2), it was found that two doublets at 47.1

Scheme 2. Structure Transformation of Complex 2 to Complex 1

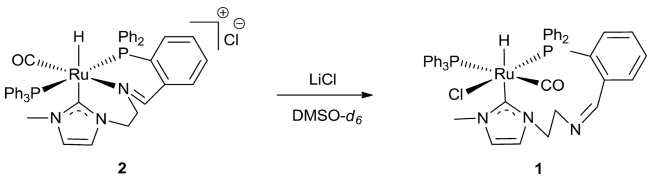

and 42.7 ppm as the characteristic signals of complex **2** were almost disappeared in the ^{31}P NMR spectrum and accompanied with the appearance of two doublets at 40.6 and 36.9 ppm, which were the same with the characteristic signals of complex **1** (Figure 3c). It clearly implied that the nitrogen

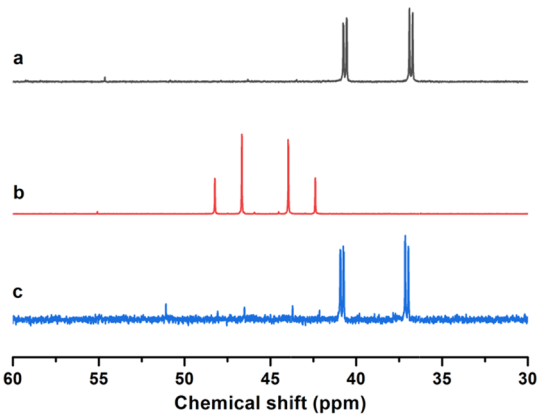

Figure 3. (a) ^{31}P NMR spectrum of complex **1**. (b) ^{31}P NMR spectrum of complex **2**. (c) ^{31}P NMR spectrum of complex **2** + 10 equiv of LiCl.

atom of imine moiety in the CNP backbone dissociated from the ruthenium center due to the competitive coordination of chloride ion with ruthenium. In other words, complex **2** could be converted to complex **1** with the increase in chloride ion concentration. This structure transformation was very similar to palladium complexes bearing **L1** reported by our group.[25]

Complex 1 Catalyzed the ADC Reaction of Alcohols to Esters. The acceptorless dehydrogenation of benzyl alcohol to afford benzyl benzoate was used as a reaction model to optimize reaction conditions. Our initial tests focused on exploring the effect of different bases and dosages of bases on the reaction (Tables S4 and S5). According to the reported results, EtONa[7b,8c] and KOtBu[7a,8b,13] were the most efficient bases for the dehydrogenative coupling of alcohols; so, we first test them and found that they were not very suitable for this system (Table 1, entries 1 and 2). Primary screening results showed that Cs_2CO_3 was the most efficient base for this reaction (entries 1−5), and increasing the amount of Cs_2CO_3 caused the yield of ester to improve obviously (entries 5−9). If no base was introduced, there was no benzoic benzoate in the system (Table 1, entry 6). The yields of benzoic benzoate decreased at temperature both higher and lower than 110 °C (Table S6). As a small amount of benzyl alcohol was not

DOI: 10.1021/acs.organomet.9b00071
Organometallics XXXX, XXX, XXX−XXX

Table 1. Effect of Bases and Complexes on the ADC of Benzyl Alcohol[a]

entry	cat. (mol %)	base (mmol)	conv (%)	yield (%)
1	**1** (1)	EtONa (0.3)	73	48
2	**1** (1)	KO^{t}Bu (0.3)	40	33
3	**1** (1)	NaO^{t}Bu (0.3)	54	47
4	**1** (1)	NaH (0.3)	63	60
5	**1** (1)	Cs_2CO_3 (0.3)	79	77
6	**1** (1)	without	2	NR[b]
7	**1** (1)	Cs_2CO_3 (0.01)	31	24
8	**1** (1)	Cs_2CO_3 (0.1)	72	70
9	**1** (1)	Cs_2CO_3 (0.5)	94	88
10[c]	**1** (0.05)	Cs_2CO_3 (0.5)	17	15
11[c]	**1** (0.1)	Cs_2CO_3 (0.5)	42	37
12[c]	**1** (0.2)	Cs_2CO_3 (0.5)	50	46
13[c]	**1** (0.5)	Cs_2CO_3 (0.5)	65	63
14[c]	**1** (1)	Cs_2CO_3 (0.5)	>99	97
15[c]	**2** (1)	Cs_2CO_3 (0.5)	97	94
16[c]	$RuHCl(CO)(PPh_3)_3$	Cs_2CO_3 (0.5)	13	6

[a]Reaction conditions: benzyl alcohol (1.0 mmol), toluene (2 mL), refluxing for 24 h. [b]NR, no reaction. [c]Reaction time: 26 h. Conversions and yields were determined by GC.

converted into ester within 24 h, the reaction time was slightly extended to 26 h, so that both the conversion and yield were increased to >99% and 97%, respectively (entries 9 and 14). The yields of esters were improved with increasing the catalyst loading from 0.05 to 1 mol % (entries 10−14), and the highest yield of ester was up to 97% with 1 mol % complex **1**. Interestingly, the catalytic performance of complex **2** was almost equivalent to that of complex **1** under the same conditions (entry 15). However, analogous complex $RuHCl(CO)(PPh_3)_3$ as a catalyst (1 mol %) gave only a low conversion of 13% (entry 16).

According to previous tests, the optimum reaction conditions were determined as 1 mol % complex **1**, 0.5 equiv of Cs_2CO_3 in 2 mL of toluene at 110 °C for 26 h. Subsequently, the scope of substrates was investigated under the optimum condition. It was found that all *para*-substituted aromatic primary alcohols, whatever they contained electron-withdrawing groups, such as $-CF_3$ and −F, or electron-donating groups, such as −Me and −OMe, showed excellent reactivity (Table 2, **3b**−**3f**). In addition, a fluorine atom at the *meta* position (**3h**) did not almost affect the conversion of substrate, but *ortho*-fluorobenzyl alcohol showed no corresponding product at all (**3k**). The result was similar with Beller's system, in which the catalyst deactivation should be attributed to the coordination of the fluorine atom at the *ortho* position with the metal center.[13] Similarly, *ortho*-chlorobenzyl alcohol (**3j**) afforded the corresponding product in a much lower yield than *para*- and *meta*-chlorine-substituted substrates (**3e** and **3g**). For *ortho*-methylbenzyl alcohol (**3i**) with a similar steric hindrance to *ortho*-fluorobenzyl and *ortho*-chlorobenzyl alcohols, a 77% yield of the product was obtained. Obviously, the major reason for the low reactivities of *ortho*-fluorobenzyl and *ortho*-chlorobenzyl alcohols should be that the F or Cl atom at the *ortho* position took part in the coordination with ruthenium species and inhibited the dehydrogenation reaction.

Notably, for the dehydrogenation coupling of cinnamyl alcohol to the corresponding ester (**3m**), its carbon−carbon double bonds in the product were hydrogenated into carbon−carbon single bonds. Next, we turned our attention to heterocyclic alcohols. For the *N*-heterocyclic substrate (**3o**), this system afforded the corresponding ester in an excellent yield of 87%. However, the conversions of O- and S-containing heterocyclic substrates (**3p** and **3q**) showed the relatively low reactivity (41% and 20%, respectively), but the yield of 3-furanmethanol to ester could be improved to 64% by extending the reaction time to 72 h. However, the conversion of 3-thiophenemethanol was still low (20%) even if the reaction time was extended to 72 or 96 h. Exceptionally, for 2-thiophenemethanol, being not reported in other systems,[6−15] a yield of 27% could be given (**3r**). A possible reason was that the coordination of an electron donor oxygen or sulfur atom in heterocycle with the ruthenium center blocked the dehydrogenation of substrates.

For alkyl primary alcohols, especially long-chain alcohols without branched chains, they were also converted in excellent yields of 90 to 95% (**3s**−**3u**). The sterically crowded derivatives 2-methylpentan-1-ol and 2-ethylbutan-1-ol presented the relatively low yields of 51 and 36% (**3v** and **3w**), respectively, but the yields were obviously improved by extending the reaction time (**3v** and **3w**). These results demonstrated that the catalytically active species in the system had good stability and long life, which could be contributed to the robust anchoring role of NHC located on a flexible pincer backbone to the ruthenium center. Furthermore, a secondary alcohol was transformed into a corresponding ketone (3×), being similar with the reported results.[12,26]

To further assess the generality of this catalytic system and to break through the limitation of substrates in most of the reported systems, an attempt was made to prepare unsymmetrical esters through dehydrogenation cross-coupling of two different primary alcohols. It was found that the desired cross-esters were obtained in moderate to good yields. Unlike the cross-esterification between substituted benzylic alcohols and linear aliphatic primary alcohols reported by Milstein et al.,[10,18] our system realized the cross-esterification between benzylic alcohols and aromatic alcohols or branched aliphatic alcohols. The reaction of *p*-methoxybenzyl alcohol (0.5 mmol) with *o*-methoxybenzyl alcohol (2 mmol) in the presence of 2 mol % of complex **1** (Table 3, entry 1) gave *o*-methoxybenzyl 4-methoxybenzoate in a yield of 59%, together with *p*-methoxybenzyl *p*-methoxybenzoate of 17%. As the amount of R_2CH_2OH was exceedingly used, the yields of self-esterification products generated from R_2CH_2OH were not listed in Table 3. In particular, the carbonyl moiety in the cross-ester was derived from the more active alcohol among two primary alcohols. Interestingly, *p*-trifluoromethylbenzyl alcohol gave two cross-esters: *p*-trifluoromethylbenzyl *p*-methoxybenzoate (**4bb**) (28%), in which the carbonyl moiety of the ester was derived from *p*-methoxybenzyl alcohol and *p*-methoxybenzyl *p*-trifluoromethylbenzoate (**4bb′**) (50%), in which the carbonyl moiety was from *p*-trifluoromethylbenzyl alcohol (Table 3, entry 2). For the reaction of *p*-methoxybenzyl alcohol with *o*-chlorobenzyl alcohol, *o*-chlorobenzyl 4-methoxybenzoate was isolated in 51% yield along with *p*-methoxybenzyl *p*-methoxybenzoate of 32% (Table 3, entry 3). Of course, a small amount of *o*-chlorobenzyl *o*-chlorobenzoate was obtained. For aliphatic alcohols, reactions of *p*-methoxybenzyl alcohol with 2-methylpentan-1-ol, 2-ethylbutan-1-ol, 2,2-dimethylpropan-1-ol, and 3-methylbutan-1-ol formed the corresponding cross-esters in yields of 51, 85, 54, and 85%, respectively (entries 4−7). The reaction of *p*-methoxybenzyl alcohol with methanol generated methyl *p*-

DOI: 10.1021/acs.organomet.9b00071
Organometallics XXXX, XXX, XXX−XXX

Table 2. Effect of Substituents on the ADC of Alcohols[a]

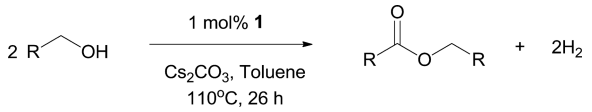

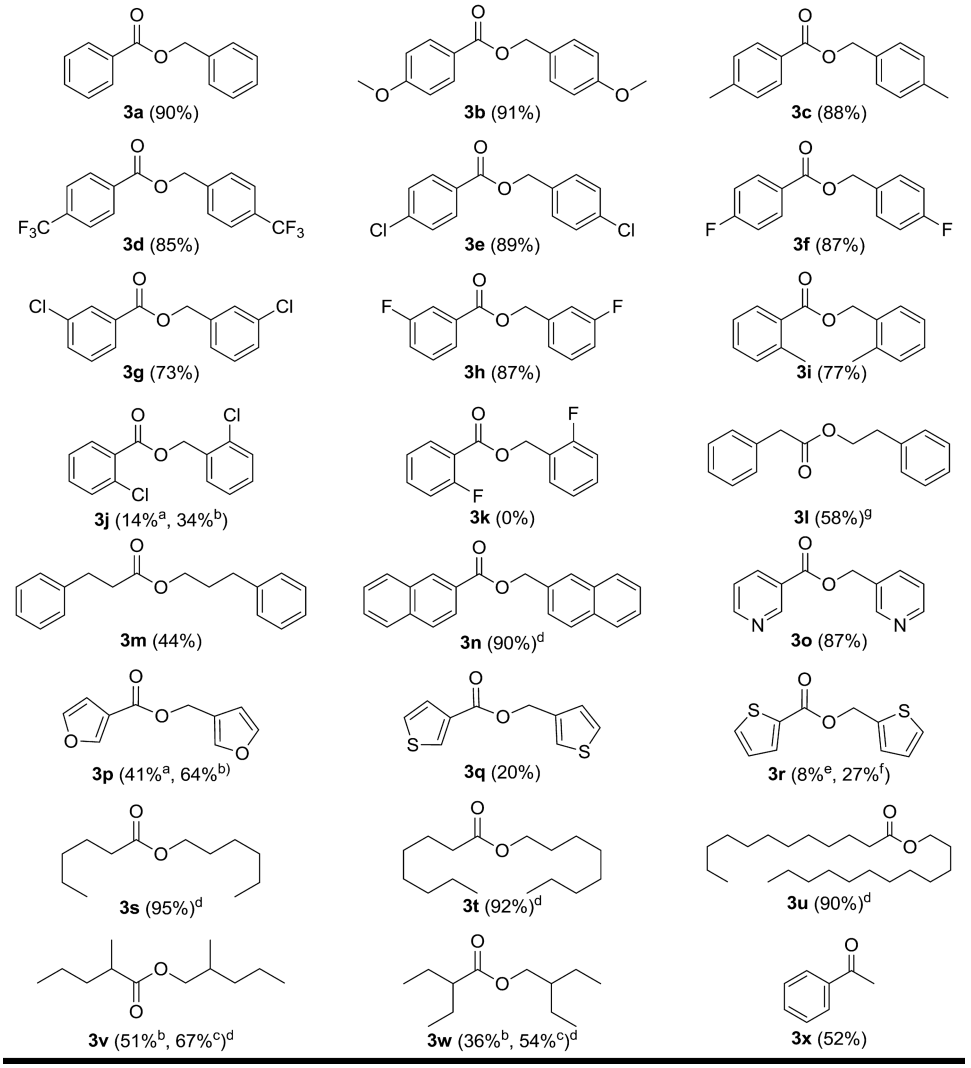

[a]Reaction conditions: benzyl alcohol (1.0 mmol), Cs_2CO_3 (0.5 mmol), complex **1** (1.0 mol %), toluene (2 mL), reaction time (26 h), N_2 balloon, and isolated yields in parentheses. [b]Reaction time: 72 h. [c]Reaction time: 96 h. [d]Yield determined by ^{1}H NMR using dibromomethane as an internal standard. [e]Catalyst (1.5 mol %), reaction time (72 h). [f]Catalyst (2.5 mol %), reaction time (72 h). [g]Yield determined by GC−MS.

methoxybenzoate yield of 37%, while the self-esterification product of *p*-methoxybenzyl alcohol was obtained in 42% yield (entry 8). For the reaction of 2-ethylbutan-1-ol with benzyl alcohol and *p*-trifluoromethylbenzyl alcohol, the cross-esterification products were obtained in good yields of 67 and 81%, respectively (entries 9 and 10). Last, primary alcohol with cyclohexanol successfully afforded the desired cross-coupling ester (entry 11).

To understand the reaction mechanism, NMR and HRMS were used to monitor the reaction process and to find some possible active species. The NMR spectra were recorded after the reaction progressed for 1 min, 10 min, 0.5 h, 1.0 h, and 2.0 h, respectively (Figures S6−S8). After 2 h, the NMR yield of ester was up to 85%. At the beginning of the reaction, the ^{31}P NMR spectrum of the reaction mixture (Figure 4a) clearly evidenced that a part of complex **1** was transformed into complex **2** under the reaction condition after 1 min. In fact, the result indicated the reason why the catalytic performance of complex **1** was very close to complex **2** (Table 1, entries 14 and 15). Subsequently, PPh_3 was completely dissociated from the ruthenium center according to the signal of ^{31}P NMR (Figure 4b) at −5 ppm after 10 min, while an available coordination site in the ruthenium center was quickly generated for the substrate. Furthermore, a doublet at 8.6 ppm in ^{1}H NMR (Figure 4c) was kept during all reaction times and indicated that the double bond C═N in the CNP backbone was not hydrogenated in the catalytic cycle. Therefore, even if there was no N−H linker, which is necessary to promote the dehydrogenation of alcohols reported by Milstein and Gusev et al.,[7,8] this system also exhibited good catalytic performance.

DOI: 10.1021/acs.organomet.9b00071
Organometallics XXXX, XXX, XXX−XXX

Table 3. Cross-Esterification between Two Different Primary Alcohols

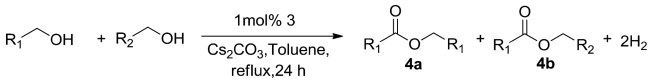

entry	R_1CH_2OH	R_2CH_2OH	Yield of **4a** (%)[a]	Yield of **4b** (%)[a]
1	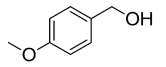	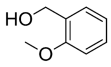	17	59 (**4ba**)
2	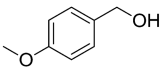	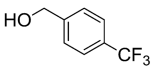	18	28(**4bb**)+50(**4bb'**)
3	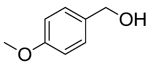	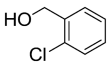	32	51 (**4bc**)
4	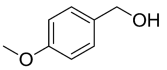	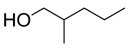	11	51(**4bd**)
5	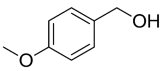	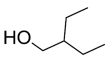	14	85 (**4be**)
6	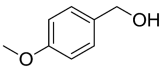		23	54 (**4bf**)
7	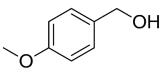	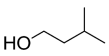	10	85 (**4bg**)
8	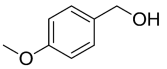	MeOH	42	37 (**4bh**)
9	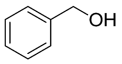	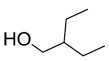	5	67[b] (**4bi**)
10	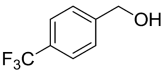	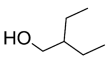	12	81 (**4bj**)
11	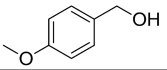		23	45 (**4bk**)

[a]Reaction conditions: R_1CH_2OH (0.5 mmol), R_2CH_2OH (2.0 mmol), Cs_2CO_3 (0.5 mmol), complex (2.0 mol %), toluene (2 mL), reflux under N_2 for 26 h, and isolated yields in parentheses. [b]Yield determined by ^1H NMR with dibromomethane as an internal standard. [c]Reaction temperature: 90 °C.

The effect of Cs_2CO_3 on the reaction showed (Table S5) that a high yield of ester could be obtained when the dosage of Cs_2CO_3 was much more than the loading of catalyst. It demonstrated that Cs_2CO_3 was involved in some essential step(s) toward ester formation other than activating the ruthenium precatalyst.[27] The appearance of the strong peak at 9.39 ppm for free PhCHO in the ^1H NMR spectrum (Figure 4d) was a direct evidence for the production of ester via aldehyde as an intermediate in this system.

According to the reported results, the ADC pathway generally undergoes dehydrogenation of alcohol to aldehyde involving dihydride ruthenium and ruthenium-benzyloxy intermediates as key active species.[6c,28] The evidences of intermediates ruthenium-benzyloxy [**3-OBn**] (*m/z* 636.1) (Figure S9) and dihydride ruthenium [**3-H**] (*m/z* 530.0) (Figure S10) were found on ESI-MS spectrum on the basis of the *m/z* values and isotopic patterns. According to in situ ^1H NMR spectra (Figure S7), two doublets at −6.93 (J = 82.5 Hz) and −7.11 ppm (J = 81.5 Hz) indicated that the hydride and phosphine moiety in the active species were mutually located in the *para* position. Probably, the NMR signals of hydride were from species **4** and **5** in Scheme 4.

In general, further conversion of aldehyde to ester involves two pathways: aldehyde reacts with another molecule of alcohol to give a hemiacetal, which finally goes through dehydrogenation into an ester.[8c,12,15,29] Alternatively, two molecules of aldehyde undergo Tishchenko reaction to form a molecule of ester.[28e,30] In order to further explore the possible route of aldehyde coupling into ester in our system, some control experiments in the presence or absence of benzyl alcohol were conducted (Scheme 3). Without benzyl alcohol and complex **1**, the coupling of benzaldehyde to the corresponding ester could not occur in the presence of Cs_2CO_3 (Scheme 3a). After 1 equiv of alcohol with respect to aldehyde was introduced into the system without complex **1**, the ester was formed in a NMR yield of 42% (Scheme 3b). Obviously, the alcohol promoted the transformation of aldehyde to ester in this system even if there was no catalyst. The result was in agreement with Gauvin's system.[6c] In our system, it might be the alkoxide, generated by reacting benzyl alcohol with alkali, that catalyzed the coupling of aldehyde to

DOI: 10.1021/acs.organomet.9b00071
Organometallics XXXX, XXX, XXX−XXX

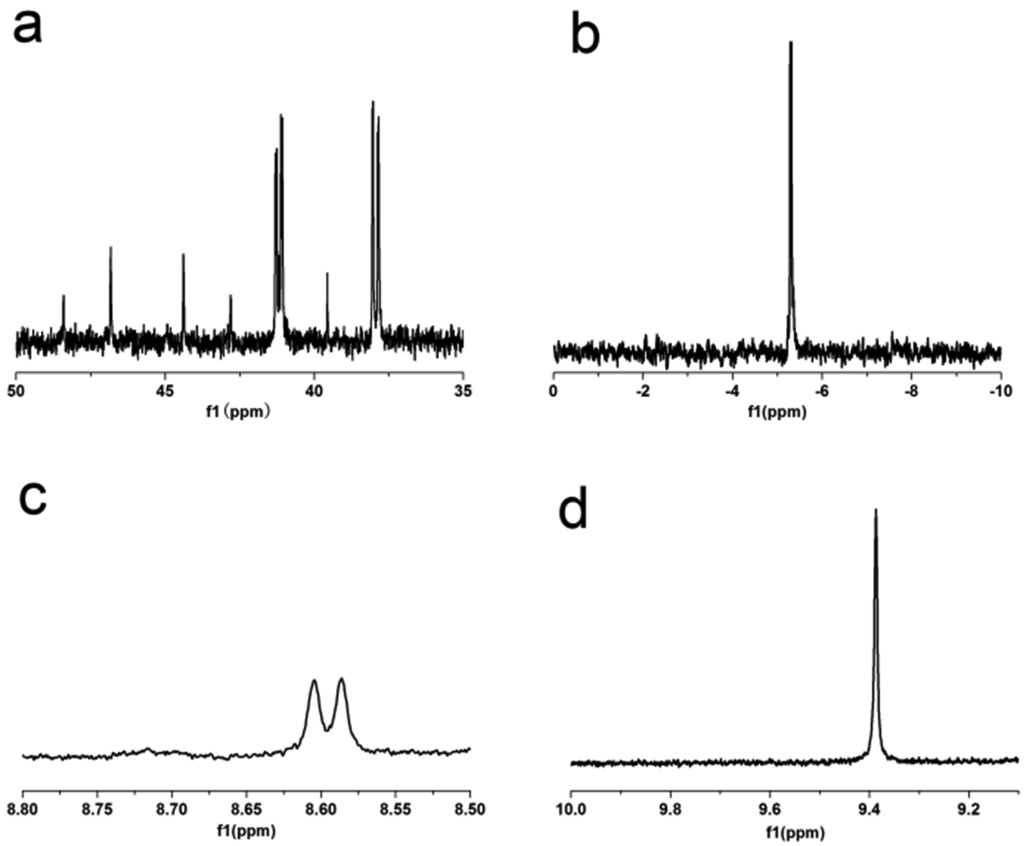

Figure 4. NMR spectra of the ADC reaction mixture. (a) ^{31}P NMR of complex **1** in the ADC reaction for 1 min. (b) ^{31}P NMR of free PPh_3 for 10 min. (c) ^{1}H NMR of —CH═N— moiety of complex **1**. (d) ^{1}H NMR of formed PhCHO.

Scheme 3. Control Experiments about Tishchenko Coupling Benzaldehyde to Benzyl Benzoate

a. Cs_2CO_3 catalyzed Tishchenko coupling of benzaldehyde to benzyl benzoate.

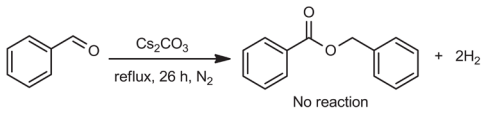

b. Cs_2CO_3 catalyzed Tishchenko coupling of benzaldehyde to benzyl benzoate in the presence of benzyl alcohol.

c. Complex **1**/Cs_2CO_3 catalyzed Tishchenko coupling of benzaldehyde to benzyl benzoate.

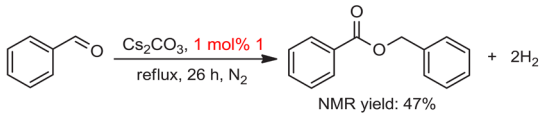

d. Complex **1**/Cs_2CO_3 catalyzed Tishchenko coupling of benzaldehyde to benzyl benzoate in the presence of benzyl alcohol.

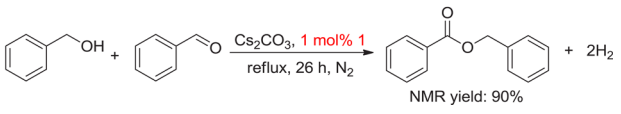

ester without a catalyst; so, the formation of ester proceeded in a Tishchenko-type mechanism. After the catalyst was added, 90% yield of benzyl benzoate was obtained with an equal ratio of benzyl alcohol to benzaldehyde (Scheme 3d). Compared with the result in the absence of catalyst, the existence of a catalyst greatly accelerated the formation of ester under the same reaction condition (Figure S11). Hence, it was suggested that the ester was generated in Tishchenko and in Ru-catalyzed hemiacetal dehydrogenation mechanisms.

Based on the previous experimental evidence, we envision plausible routes as illustrated in Scheme 4. At the onset of catalysis, complex **1** was rapidly converted into complex **2** under the reaction condition. Upon the combination of complex **2** with alcohol, it was accompanied with the dissociation of PPh_3 from complex **2**. Benzyloxy, generated by the deprotonation of benzyl alcohol in the presence of a base, subsequently combined with ruthenium species to form ruthenium-benzyloxy species **3-OBn** (Scheme 4, cycle A). **3-OBn** went through a β-hydride elimination step to give benzaldehyde and dihydride ruthenium species **3-H** that was observed in HRMS (Figure S10) and ^{1}H NMR (Figure S7c). The catalytic cycle was accomplished by the release of H_2 to regenerate species **3**. After benzaldehyde was formed, it went through two parallel routes to form ester (Scheme 4, cycles B and C). One route involved the Tishchenko-type pathway mediated by **3-OBn**. It passed through two consecutive nucleophilic additions and 1,3-hydride migration (Scheme 4, path I). Alternatively, the hemiacetal formed from the reaction between benzaldehyde and benzyl alcohol was dehydrogenated by Ru−H species **3** via **5** to give ester (, Scheme 4, path II).

DOI: 10.1021/acs.organomet.9b00071
Organometallics XXXX, XXX, XXX−XXX

Scheme 4. Proposed Mechanism

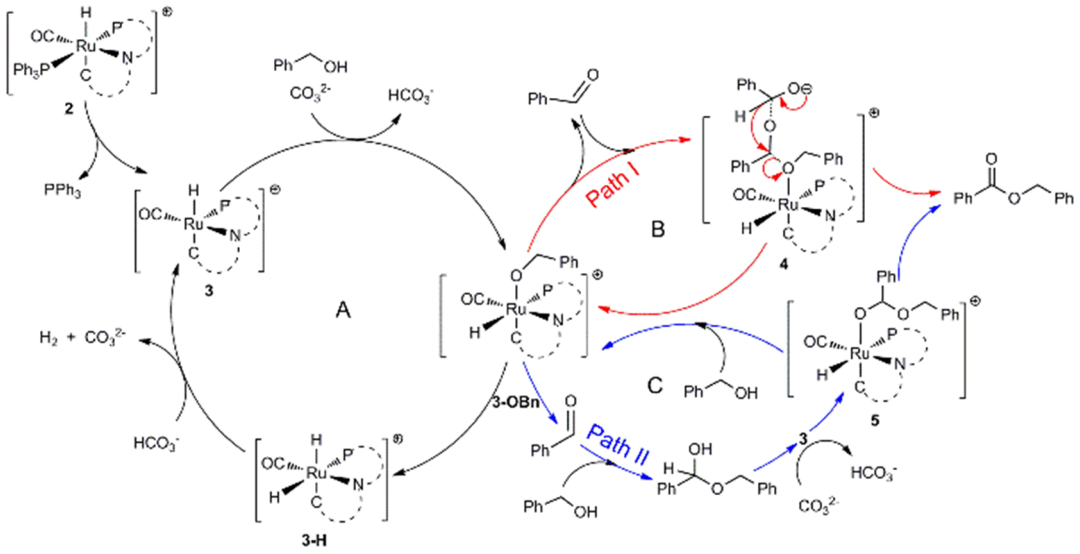

CONCLUSIONS

In summary, we synthesized and characterized two novel hemilabile ruthenium complexes RuH(CO)Cl(PPh_3)(κ^2-CP) (**1**) and [*fac*-RuH(CO)(PPh_3)(κ^3-CNP)]Cl (**2**) bearing an unsymmetrical flexible pincer ligand CNP ($\mathbf{L_1}$). Complex **1** and **2** were isomers for each other, and complex **1** could be formed by adding chloride ions to the solution of complex **2**. For the first time, the facial ruthenium(II) complexes bearing an unsymmetrical *N*-heterocyclic carbene−nitrogen−phosphine (CNP) ligand were successfully applied in the acceptorless dehydrogenative coupling of alcohols to esters. The activity of complex **1** was comparable to that of complex **2**. Good-to-excellent yields were gained in the case of *para*-substituted benzyl alcohols and long-chain primary alcohols as substrates. Moreover, the steric hindrance of the *ortho* substituent in substrates also slightly affects the reactivity of substrates, while the electronic factor of substrates did not lead to a remarkable influence on the reaction. However, for substrates with an electron donor (F, Cl) at the *ortho* position, the coordination of the electron donor at the *ortho* position with ruthenium species resulted in the low reactivity of substrates. Especially, the system carried out acceptorless dehydrogenation to generate cross-esters in moderate-to-good yields with two different primary alcohols.

EXPERIMENTAL SECTION

General Methods and Instrumentation. All operations were performed in the nitrogen atmosphere or glovebox. All solvents were purified with standard methods. Reagents were purchased from commercial suppliers and used as-received. RuHCl(CO)(PPh_3)$_3$[31] and 3-{2-{[2-(diphenylphosphino)-benzylidene]amino}ethyl}-1-methyl-1*H*-imidazol-3-ium chloride ($\mathbf{L_1}$)[25] were synthesized with the reported methods. ^{1}H NMR, ^{13}C NMR, ^{31}P NMR, and ^{1}H-^{13}CHMQC spectra were measured on the Bruker AVANCE III HD 400 MHz. GC analysis was carried out with Agilent 7890B (KB-1, 30 m × 0.32 mm × 0.25 μm). HRMS was recorded on a SHIMADZU LCMS-IT-TOF mass spectrometer.

X-Ray Crystallographic Details. Single-crystal X-ray diffraction was performed on a Xcalibur Eos X-ray single-crystal diffractometer at 293(2) K. The structure was solved by Olex2[32] with the ShelXS[33] structure solution program using direct methods and refined with the ShelXL[34] refinement package (least squares minimization).

Synthesis of RuH(CO)Cl(PPh_3)(κ^2-CP) (1). The mixture of $\mathbf{L_1}$ (2 mmol, 866.2 mg) and silver oxide (1.1 mmol, 255.2 mg) in dichloromethane (10 mL) was stirred at room temperature for 2 h. Then, the solution was filtered with Celite and 30 mL of anhydrous diethyl ether was added into the filtrate to precipitate a pale yellow solid. The solid was filtered, washed with ether (10 mL) three times, and dried under vacuum to give pale yellow powder. Subsequently, the pale yellow powder (0.1 mmol, 54.1 mg), RuHCl(CO)(PPh_3)$_3$ (0.1 mmol, 95.1 mg) was dissolved in toluene (15 mL) in a two-necked flask. After the mixture was stirred at 60 °C for 3 h, it was filtered, washed with toluene and *n*-hexane successively, and dried in vacuum to give a pale brown solid. The crude product was purified by column chromatography to give pure complex **1** (45.4 mg, 55% yield). ^{1}H NMR (CD_2Cl_2, 400.1 MHz, δ): 8.63 (s, 1H), 7.49 (m, 2H), 6.8−7.4 (m, 26H), 6.58 (s, 1H), 6.20 (t, 2H, J = 8.0 Hz), 4.39−4.52 (m, 2H), 4.02 (d, 1H, J = 12.0 Hz), 3.89 (s, 3H), 2.59 (t, 1H, J = 8.0 Hz), −12.04 (dd, J = 24.2, 14.3 Hz, 1H). ^{31}P NMR (CD_2Cl_2, 162.0 MHz, δ): 40.7 (dd, $J_{P\text{-}P}$ = 30.8 Hz, $J_{P\text{-}H}$ = 4.9 Hz), 36.8 (dd, $J_{P\text{-}P}$ = 30.8 Hz, $J_{P\text{-}H}$ = 3.2 Hz). HRMS (ESI-TOF) *m/z*: [M-Cl]$^+$ calcd for $C_{44}H_{40}N_3OP_2Ru$, 790.1690; found, 790.1665; [M-Cl-PPh_3]$^+$ calcd for $C_{26}H_{25}N_3OPRu$, 528.0779; found 528.0774; [M-Cl-PPh_3-CO]$^+$ calcd for $C_{25}H_{25}N_3PRu$, 500.0830; found, 500.0823.

Synthesis of [*fac*-RuH(CO)(PPh_3)(κ^3-CNP)]Cl (2). The pale yellow powder (0.1 mmol, 54.1 mg) obtained by reacting $\mathbf{L_1}$ and Ag_2O, and RuHCl(CO)(PPh_3)$_3$ (0.1 mmol, 95.1 mg) was dissolved in tetrahydrofuran (15 mL) in a 50 mL two-necked flask with a reflux condenser. The mixture was refluxed for 5 h and filtered. The solvent of the filtrate was reduced to about 5 mL under vacuum, and then 30 mL of *n*-hexane was added into it, and a brownish yellow solid was precipitated. The precipitate was filtered, washed with *n*-hexane (10 mL) three times, and dried in vacuum to give a pale brown solid. This crude product was purified by anhydrous anaerobic chromatography column with dichloromethane/methanol (10:1) as eluent to give complex **2** (38.2 mg, 46%). Single crystals suitable for X-ray diffraction were obtained by diffusing *n*-hexane into dichloromethane solution of complex **2**. ^{1}H NMR (CD_2Cl_2, 400.1 MHz, δ): 8.64 (s, 1H), 7.83 (m, 1H), 6.77−7.64 (m, 28H), 6.45 (t, 2H, J = 8.0 Hz), 3.99 (d, 1H, J = 16.0 Hz), 3.61 (d, 1H, J = 12.0 Hz), 3.47 (t, 1H, J = 12.0 Hz), 2.96 (s, 3H), 2.31 (t, 1H, J = 12.0 Hz), −7.55 (dd, J = 24.8, 22.0 Hz, 1H). ^{13}C NMR (CD_2Cl_2, 100.6 MHz, δ): 207.83, 183.37, 171.24 (d, J = 7.0 Hz), 137.39 (d, J = 13.1 Hz), 135.28 (d, J = 8.0 Hz), 134.46 (d, J = 3.0 Hz), 134.28, 134.07 (d, J = 3.0 Hz), 133.80, 132.94 (d, J = 10.1 Hz), 132.66 (d, J = 6.0 Hz), 132.33, 132.06, 131.89 (d, J = 10.1 Hz), 131.04, 130.93, 130.81, 130.37, 130.05, 128.74 (t, J = 10.1 Hz), 128.55 (d, J = 9.1 Hz), 123.44, 122.72, 65.52 (d, J = 4.0 Hz), 51.89, 38.83. ^{31}P NMR (CD_2Cl_2, 162.0 MHz, δ): 47.0

DOI: 10.1021/acs.organomet.9b00071
Organometallics XXXX, XXX, XXX−XXX

(d, J_{P-P} = 254.3 Hz), 42.7 (d, J_{P-P} = 254.3 Hz). HRMS (ESI-TOF) *m/z*: $[M-Cl]^+$ calcd for $C_{44}H_{40}N_3OP_2Ru$, 790.1690; found, 790.1681; $[M-Cl-PPh_3]^+$ calcd for $C_{26}H_{25}N_3OPRu$, 528.0779; found, 528.0761.

Typical Procedure for the ADC of Alcohols. After complex **1** (0.01 mmol, 8.3 mg), Cs_2CO_3 (0.5 mmol, 162.9 mg) were added to a dry Schlenk tube in the glovebox, benzyl alcohol (1.0 mmol, 104 μL) and anhydrous toluene (2 mL) were sequentially injected into the tube. The solution was refluxed with stirring for 26 h. At the end of the reaction, the mixture was cooled to room temperature and diluted with 2 mL of dichloromethane and filtered with Celite. The filtrate was evaporated to dry, and the product was separated by column chromatography to give a light yellow liquid **3a** (95.5 mg, 90%).

■ ASSOCIATED CONTENT

Supporting Information

The Supporting Information is available free of charge on the ACS Publications website at DOI: 10.1021/acs.organomet.9b00071.

Optimization of the ADC reaction conditions, crystal data for complex **2**, mechanistic study, and NMR spectra (PDF)

Accession Codes

CCDC 1904695 contains the supplementary crystallographic data for this paper. These data can be obtained free of charge via www.ccdc.cam.ac.uk/data_request/cif, or by emailing data_request@ccdc.cam.ac.uk, or by contacting The Cambridge Crystallographic Data Centre, 12 Union Road, Cambridge CB2 1EZ, UK; fax: +44 1223 336033.

■ AUTHOR INFORMATION

Corresponding Authors

*E-mail: liruixiang@scu.edu.cn (R.L.).
*E-mail: scucqxjyu@163.com (X.Y.).

ORCID

Haiyan Fu: 0000-0002-7185-2062
Xueli Zheng: 0000-0001-8394-0310
Hua Chen: 0000-0003-4248-8019
Ruixiang Li: 0000-0003-0756-3722

Notes

The authors declare no competing financial interest.

■ ACKNOWLEDGMENTS

This work was financially supported by the National Natural Science Foundation of China (21572137 and 21871187) and the Key Program of Sichuan Science and Technology Project (nos. 2018GZ0312 and 2019YFG0146) and the Sichuan University Innovation Spark research fund (no. 2018SCUH0079).

■ REFERENCES

(1) (a) Ogliaruso, M. A.; Wolfe, J. F. *Synthesis of Carboxylic Acids, Esters and Their Derivatives*; John Wiley & Sons Ltd: Hoboken, NJ, 1991. (b) Larock, R. C. *Comprehensive Organic Transformations*; VCH: New York, 1989.

(2) (a) Choi, J.-H.; Choi, J.-Y.; Kim, E.-M.; Kim, J.-P.; Towns, A. D.; Yoon, C. Coloration properties and clearability of phthalimide-derived monoazo disperse dyes containing ester groups. *Color. Technol.* **2013**, *129*, 352−359. (b) Singh, S. P.; Sing, D. Biodiesel production through the use of different sources and characterization of oils and their esters as the substitute of diesel: A review. *Renewable Sustainable Energy Rev.* **2010**, *14*, 200−216. (c) Otera, J. *Esterification: Methods, Reactions, and Applications*, Wiley-VCH, Weinheim, 2003.

(3) (a) Tana, T.; Guo, X.-W.; Xiao, Q.; Huang, Y.; Sarina, S.; Christopher, P.; Jia, J.; Wu, H.; Zhu, H. Non-plasmonic metal nanoparticles as visible light photocatalysts for the selective oxidation of aliphatic alcohols with molecular oxygen at near ambient conditions. *Chem. Commun.* **2016**, *52*, 11567−11570. (b) Davis, S. E.; Ide, M. S.; Davis, R. J. Selective oxidation of alcohols and aldehydes over supported metal nanoparticles. *Green Chem.* **2013**, *15*, 17−45.

(4) (a) Murahashi, S. I.; Ito, K. I.; Naota, T.; Maeda, Y. Ruthenium catalyzed transformation of alcohols to esters and lactones. *Tetrahedron Lett.* **1981**, *22*, 5327−5330. (b) Blum, Y.; Shvo, Y. Catalytically reactive (η^4-tetracyclone) $(CO)_2(H)_2Ru$ and related complexes in dehydrogenation of alcohols to esters. *J. Organomet. Chem.* **1985**, *282*, C7−C10.

(5) (a) Werkmeister, S.; Neumann, J.; Junge, K.; Beller, M. Pincer-Type Complexes for Catalytic (De) Hydrogenation and Transfer (De) Hydrogenation Reactions: Recent Progress. *Chem. − Eur. J.* **2015**, *21*, 12226−12250. (b) Gunanathan, C.; Milstein, D. Bond activation and catalysis by ruthenium pincer complexes. *Chem. Rev.* **2014**, *114*, 12024−12087.

(6) (a) Zhang, J.; Leitus, G.; Ben-David, Y.; Milstein, D. Facile conversion of alcohols into esters and dihydrogen catalyzed by new ruthenium complexes. *J. Am. Chem. Soc.* **2005**, *127*, 10840−10841. (b) Gusev, D. G. Dehydrogenative coupling of ethanol and ester hydrogenation catalyzed by pincer-type YNP complexes. *ACS Catal.* **2016**, *6*, 6967−6981. (c) Nguyen, D. H.; Trivelli, X.; Capet, F.; Swesi, Y.; Favre-Réguillon, A.; Vanoye, L.; Dumeignil, F.; Gauvin, R. M. Deeper mechanistic insight into Ru pincer-mediated acceptorless dehydrogenative coupling of alcohols: exchanges, intermediates and deactivation species. *ACS Catal.* **2018**, *8*, 4719−4734. (d) Vicent, C.; Gusev, D. G. ESI-MS insights into acceptorless dehydrogenative coupling of alcohols. *ACS Catal.* **2016**, *6*, 3301−3309.

(7) (a) Bertoli, M.; Choualeb, A.; Lough, A. J.; Moore, B.; Spasyuk, D.; Gusev, D. G. Osmium and ruthenium catalysts for dehydrogenation of alcohols. *Organometallics* **2011**, *30*, 3479−3482. (b) Spasyuk, D.; Gusev, D. G. Acceptorless dehydrogenative coupling of ethanol and hydrogenation of esters and imines. *Organometallics* **2012**, *31*, 5239−5242. (c) Spasyuk, D.; Vicent, C.; Gusev, D. G. Chemoselective hydrogenation of carbonyl compounds and acceptorless dehydrogenative coupling of alcohols. *J. Am. Chem. Soc.* **2015**, *137*, 3743−3746.

(8) (a) Zhang, J.; Balaraman, E.; Leitus, G.; Milstein, D. Electron-rich PNP- and PNN-type ruthenium(II) hydrido borohydride pincer complexes. Synthesis, structure, and catalytic dehydrogenation of alcohols and hydrogenation of esters. *Organometallics* **2011**, *30*, 5716−5724. (b) Fogler, E.; Garg, J. A.; Hu, P.; Leitus, G.; Shimon, L. J. W.; Milstein, D. System with potential dual modes of metal−ligand cooperation: highly catalytically active pyridine-based PNNH−Ru pincer complexes. *Chem. − Eur. J.* **2014**, *20*, 15727−15731. (c) Nielsen, M.; Junge, H.; Kammer, A.; Beller, M. Towards a green process for bulk-scale synthesis of ethyl acetate: Efficient acceptorless dehydrogenation of ethanol. *Angew. Chem.* **2012**, *124*, 5809−5811. (d) Musa, S.; Fronton, S.; Vaccaro, L.; Gelman, D. Bifunctional ruthenium (II) PCP pincer complexes and their catalytic activity in acceptorless dehydrogenative reactions. *Organometallics* **2013**, *32*, 3069−3073. (e) Zhang, L.; Raffa, G.; Nguyen, D. H.; Swesi, Y.; Corbel-Demailly, L.; Capet, F.; Trivelli, X.; Desset, S.; Paul, S.; Paul, J.-F.; Fongarland, P.; Dumeignil, F.; Gauvin, R. M. Acceptorless dehydrogenative coupling of alcohols catalysed by ruthenium PNP complexes: Influence of catalyst structure and of hydrogen mass transfer. *J. Catal.* **2016**, *340*, 331−343.

(9) Bertoli, M.; Choualeb, A.; Gusev, D. G; Lough, A. J.; Major, Q.; Moore, B. PNP pincer osmium polyhydrides for catalytic dehydrogenation of primary alcohols. *Dalton Trans.* **2011**, *40*, 8941−8949.

(10) Cheng, J.; Zhu, M.; Wang, C.; Li, J.; Jiang, X.; Wei, Y.; Tang, W.; Xue, D.; Xiao, J. Chemoselective dehydrogenative esterification of aldehydes and alcohols with a dimeric rhodium (II) catalyst. *Chem. Sci.* **2016**, *7*, 4428−4434.

DOI: 10.1021/acs.organomet.9b00071
Organometallics XXXX, XXX, XXX−XXX

(11) Musa, S.; Shaposhnikov, I.; Cohen, S.; Gelman, D. Ligand–metal cooperation in PCP pincer complexes: Rational design and catalytic activity in acceptorless dehydrogenation of alcohols. *Angew. Chem., Int. Ed.* **2011**, *50*, 3533–3537.
(12) Chakraborty, S.; Lagaditis, P. O.; Förster, M.; Bielinski, E. A.; Hazari, N.; Holthausen, M. C.; Jones, W. D.; Schneider, S. Well-defined iron catalysts for the acceptorless reversible dehydrogenation-hydrogenation of alcohols and ketones. *ACS Catal.* **2014**, *4*, 3994–4003.
(13) Paudel, K.; Pandey, B.; Xu, S.; Taylor, D. K.; Tyer, D. L.; Torres, C. L.; Gallagher, S.; Kong, L.; Ding, K. Cobalt-catalyzed acceptorless dehydrogenative coupling of primary alcohols to esters. *Org. Lett.* **2018**, *20*, 4478–4481.
(14) Chakraborty, S.; Piszel, P. E.; Brennessel, W. W.; Jones, W. D. A single nickel catalyst for the acceptorless dehydrogenation of alcohols and hydrogenation of carbonyl compounds. *Organometallics* **2015**, *34*, 5203–5206.
(15) Nguyen, D. H.; Trivelli, X.; Capet, F.; Paul, J.-F.; Dumeignil, F.; Gauvin, R. M. Manganese pincer complexes for the base-free, acceptorless dehydrogenative coupling of alcohols to esters: Development, scope, and understanding. *ACS Catal.* **2017**, *7*, 2022–2032.
(16) (a) Gunanathan, C.; Milstein, D. Metal-ligand cooperation by aromatization-dearomatization: A new paradigm in bond activation and "green" catalysis. *Acc. Chem. Res.* **2011**, *44*, 588–602. (b) Khusnutdinova, J. R.; Milstein, D. Metal–ligand cooperation. *Angew. Chem., Int. Ed.* **2015**, *54*, 12236–12273.
(17) Srimani, D.; Balaraman, E.; Gnanaprakasam, B.; Ben-David, Y.; Milstein, D. Ruthenium pincer-catalyzed cross-dehydrogenative coupling of primary alcohols with secondary alcohols under neutral conditions. *Adv. Synth. Catal.* **2012**, *354*, 2403–2406.
(18) Das, U. K.; Ben-David, Y.; Leitus, G.; Diskin-Posner, Y.; Milstein, D. Dehydrogenative cross-coupling of primary alcohols to form cross-esters catalyzed by a manganese pincer complex. *ACS Catal.* **2019**, *9*, 479–484.
(19) (a) Kühl, O. *Functionalised N-heterocyclic carbene complexes*; Wiley: Chichester, U. K., 2010. (b) Herrmann, W. A. N-heterocyclic carbenes: A New Concept in organometallic catalysis. *Angew. Chem., Int. Ed.* **2002**, *41*, 1290–1309.
(20) (a) Bader, A.; Lindner, E. Coordination chemistry and catalysis with hemilabile oxygen-phosphorus ligands. *Coord. Chem. Rev.* **1991**, *108*, 27–110. (b) Braunstein, P.; Naud, F. Hemilability of hybrid ligands and the coordination chemistry of oxazoline-based systems. *Angew. Chem., Int. Ed.* **2001**, *40*, 680–699. (c) Zhong, R.; Lindhorst, A. C.; Groche, F. J.; Kühn, F. E. Immobilization of N-heterocyclic carbene compounds: A synthetic perspective. *Chem. Rev.* **2017**, *117*, 1970–2058.
(21) (a) Nair, A. G.; Mcburney, R. T.; Walker, D. B.; Page, M. J.; Gatus, M. R. D.; Bhadbhade, M.; Messerle, B. A. Ruthenium(II) complexes of hemilabile pincer ligands: synthesis and catalysing the transfer hydrogenation of ketones. *Dalton Trans.* **2016**, *45*, 14335. (b) Liu, B.; Yan, J.; Huang, R.; Wang, W.; Jin, Z.; Zanoni, G.; Zheng, P.; Yang, S.; Chi, Y. R. Kinetic resolution of 1,2-diols via NHC-catalyzed site-selective esterification. *Org. Lett.* **2018**, *20*, 3447–3450. (c) Filonenko, G. A.; Aguila, M. J. B.; Schulpen, E. N.; van Putten, R.; Wiecko, J.; Müller, C.; Lefort, L.; Hensen, E. J. M.; Pidko, E. A. Bis-N-heterocyclic carbene aminopincer ligands enable high activity in Ru-catalyzed ester hydrogenation. *J. Am. Chem. Soc.* **2015**, *137*, 7620–7623.
(22) (a) Sanz, S.; Azua, A.; Peris, E. '(η^6-Arene)Ru(Bis-NHC)' complexes for the reduction of CO_2 to formate with hydrogen and by transfer hydrogenation with *i*PrOH. *Dalton Trans.* **2010**, *39*, 6339–6343. (b) Azua, A.; Sanz, S.; Peris, E. Water-soluble Ir^{III} N-heterocyclic carbene based catalysts for the reduction of CO_2 to formate by transfer hydrogenation and the deuteration of aryl amines in water. *Chem. - Eur. J.* **2011**, *17*, 3963–3967.
(23) (a) Guo, X.-Q.; Wang, Y.-N.; Wang, D.; Cai, L.-H.; Chen, Z.-X.; Hou, X.-F. Palladium, iridium and ruthenium complexes with acyclic imino-N-heterocyclic carbenes and their application in aquaphase Suzuki–Miyaura cross-coupling reaction and transfer hydrogenation. *Dalton Trans.* **2012**, *41*, 14557–14567. (b) Peris, E.; Crabtree, R. H. Recent homogeneous catalytic applications of chelate and pincer N-heterocyclic carbenes. *Coord. Chem. Rev.* **2004**, *248*, 2239–2246.
(24) (a) Leigh, V.; Ghattas, W.; Mueller-Bunz, H.; Albrecht, M. Synthesis of pincer-type N-heterocyclic carbene palladium complexes with a hemilabile ligand and their application in cross-coupling catalysis. *J. Organomet. Chem.* **2014**, *771*, 33–39.
(25) Li, Y.; Yu, X.; Wang, Y.; Fu, H.; Zheng, X.; Chen, H.; Li, R. Unsymmetrical pincer N-heterocyclic carbine-nitrogen-phosphine chelated palladium(II) complexes: synthesis, structure, and reactivity in direct Csp^2-H arylation of benzoxazoles. *Organometallics* **2018**, *37*, 979–988.
(26) (a) Chang, W.; Gong, X.; Wang, S.; Xiao, L.-P.; Song, G. Acceptorless dehydrogenation and dehydrogenative coupling of alcohols catalysed by protic NHC ruthenium complexes. *Org. Biomol. Chem.* **2017**, *15*, 3466–3471. (b) Xu, S.; Alhthlol, L. M.; Paudel, K.; Reinheimer, E.; Tyer, D. L.; Taylor, D. K.; Smith, A. M.; Holzmann, J.; Lozano, E.; Ding, K. Tripodal N,P Mixed-donor ligands and their cobalt complexes: efficient catalysts for acceptorless dehydrogenation of secondary alcohols. *Inorg. Chem.* **2018**, *57*, 2394–2397.
(27) Aviel, A.; Schelwies, M.; Schwaben, J.; Rominger, F.; Hashmi, A. S. K.; Schaub, T. Study of precatalyst degradation leading to the discovery of a new Ru^0 precatalyst for hydrogenation and dehydrogenation. *Organometallics* **2018**, *37*, 2193–2201.
(28) (a) Gunanathan, C.; Milstein, D. Applications of acceptorless dehydrogenation and related transformations in chemical synthesis. *Science* **2013**, *341*, 1229712. (b) Guillena, G.; Ramón, D. J.; Yus, M. Hydrogen autotransfer in the *N*-alkylation of amines and related compounds using alcohols and amines as electrophiles. *Chem. Rev.* **2010**, *110*, 1611–1641. (c) Obora, Y. Recent advances in α-alkylation reactions using alcohols with hydrogen borrowing methodologies. *ACS Catal.* **2014**, *4*, 3972–3981. (d) Yang, Q.; Wang, Q.; Yu, Z. Substitution of alcohols by N-nucleophiles via transition metal-catalyzed dehydrogenation. *Chem. Soc. Rev.* **2015**, *44*, 2305–2329. (e) Dobereiner, G. E.; Crabtree, R. H. Dehydrogenation as a substrate-activating strategy in homogeneous transition-metal catalysis. *Chem. Rev.* **2010**, *110*, 681–703.
(29) (a) Zweifel, T.; Naubron, J. V.; Büttner, T.; Ott, T.; Grützmacher, H. Ethanol as hydrogen donor: highly efficient transfer hydrogenations with rhodium (I) amides. *Angew. Chem., Int. Ed.* **2008**, *47*, 3245–3249. (b) Younus, H. A.; Su, W.; Ahmad, N.; Chen, S.; Verpoort, F. Ruthenium pincer complexes: synthesis and catalytic applications. *Adv. Synth. Catal.* **2015**, *357*, 283–330. (c) Alberico, E.; Lennox, A. J. J.; Vogt, L. K.; Jiao, H.; Baumann, W.; Drexler, H. J.; et al. Unravelling the mechanism of basic aqueous methanol dehydrogenation catalyzed by Ru-PNP pincer complexes. *J. Am. Chem. Soc.* **2016**, *138*, 14890–14904. (d) Sahoo, A. R.; Jiang, F.; Bruneau, C.; Sharma, G. V. M.; Suresh, S.; Roisnel, T.; Dorcet, V.; Achard, M. Phosphine-pyridonate ligands containing octahedral ruthenium complexes: access to esters and formic acid. *Catal. Sci. Technol.* **2017**, *7*, 3492–3498.
(30) (a) Ito, T.; Horino, H.; Koshiro, Y.; Yamamoto, A. Selective dimerization of aldehydes to esters catalyzed by hydridoruthenium complexes. *Bull. Chem. Soc. Jpn.* **1982**, *55*, 504–512. (b) Grushin, V. V.; Alper, H. Homogeneous metal-catalyzed sequential Rosenmund-Tishchenko reactions. *J. Org. Chem.* **1991**, *56*, 5159–5161. (c) Sorkau, A.; Schwarzer, K.; Wagner, C.; Poetsch, E.; Steinborn, D. Dimerization and cyclotrimerization of aldehydes: ruthenium catalyzed formation of esters, 1,3,5-trioxanes, and aldol condensation products from aldehydes. *J. Mol. Catal. A: Chem.* **2004**, *224*, 105–109. (d) Simon, M. O.; Darses, S. Anin situGenerated ruthenium catalyst for the Tishchenko reaction. *Adv. Synth. Catal.* **2010**, *352*, 305–308. (e) Morris, S. A.; Gusev, D. G. Rethinking the Claisen-Tishchenko reaction. *Angew. Chem., Int. Ed.* **2017**, *56*, 6228–6231.
(31) Hallman, P. S.; Mcgarvey, B. R.; Wilkinson, G. The preparation and reactions of hydridochlorotris (triphenylphosphine) ruthenium (II) including homogeneous catalytic hydrogenation of alk-1-enes. *J. Chem. Soc. A.* **1968**, 3143–3150.

DOI: 10.1021/acs.organomet.9b00071
Organometallics XXXX, XXX, XXX–XXX

(32) Dolomanov, O. V.; Bourhis, L. J.; Gildea, R. J.; Howard, J. A. K.; Puschmann, H. OLEX2: A complete structure solution, refinement and analysis program. *J. Appl. Crystallogr.* **2009**, *42*, 339−341.
(33) Sheldrick, G. M. A short history of SHELX. *Acta Cryst.* **2008**, *64*, 112−122.
(34) Sheldrick, G. M. Crystal Structure Refinement with SHELXL. *Acta Cryst. C* **2015**, *71*, 3−8.

DOI: 10.1021/acs.organomet.9b00071
Organometallics XXXX, XXX, XXX−XXX